JOURNAL OF Materials CHEMISTRY

Electronic absorption spectroscopy and colour of chromium-doped solids

Radostin S. Pavlov,* Vicente B. Marzá and Juan B. Carda

Universidad Jaume I, Campus de Riu Sec, Area Científico-Técnica, QIO, 12071 Castellón, Spain

Received 19th February 2002, Accepted 14th June 2002
First published as an Advance Article on the web 30th July 2002

Twenty-one chromium-containing compounds and solid solutions belonging to ten structural types were obtained by either solid-state reactions or the Pechini method and studied from the point of view of the relationship between structure, composition and colour. Formation of single-phase products was assured by heating on several high-temperature stages and monitoring phase transformations by X-ray diffraction. Electronic absorption spectra and colour coordinates of the samples were obtained and analysed paying special attention to the dependence of the colour on the structural characteristics and the presence of chromium in oxidation states other than Cr(III).

Introduction

At present, there is an increasing need to develop new highly stable red-shade ceramic pigments, as a result of the implementation of new technologies and new environmental requirements. Existing cadmium sulfoselenide red pigments ($CdS_{1-x}Se_x$) present rather good chromatic properties, but their thermal stability is unsatisfactory.[1] Moreover, they are suspected of possessing carcinogenic properties and their manufacture involves the formation of toxic emissions.[2,3]

Chromium-based pigments could turn out to be a safe alternative to the sulfoselenide, although no chromium pigment has been discovered so far that shows a red shade of similar intensity in combination with a better thermal stability. The search for a pigment of such characteristics, led to the present study, which is an attempt to revise and systematize the knowledge about the mechanism of colouration of chromium-doped solids.

Usually the colour of the chromium-doped materials is explained by the formalism of the crystal field theory applied to Cr(III). It has d^3 electronic configuration and in oxides prefers octahedral coordination. Several electronic transitions are possible in this case and they are given in Table 1 together with the labels most commonly applied to the corresponding absorption bands.[4]

All of these transitions are forbidden by Laporte's selection rule due to the equal parity of the ground and the excited state (g). However, the prohibition imposed by this rule is partially relaxed by the presence of odd-parity crystal fields and odd-parity nuclear vibrations. In addition, the transitions corresponding to the R, R′ and B bands are spin-forbidden and the one corresponding to the Y′ band supposes a two-electron jump in the strong field limit, which is also forbidden. The spin selection rule is slightly released by spin–orbit interactions and therefore the R and R′ bands are observed, although less intense than the bands Y and U, which are due to parity-only-forbidden transitions. The intensity of the Y′band is enhanced by configuration mixing of the states $^4T_{1g}$ (^4F) and $^4T_{1g}$ (^4P).

Table 1 Transitions of Cr(III) in octahedral crystal field and lables used for their corresponding bands

Transition	Band
$^4A_{2g} \rightarrow {}^2E_g$ (^2G)	R
$^4A_{2g} \rightarrow {}^2T_{1g}$ (^2G)	R′
$^4A_{2g} \rightarrow {}^4T_{2g}$ (^4F)	U
$^4A_{2g} \rightarrow {}^2T_{2g}$ (^2G)	B
$^4A_{2g} \rightarrow {}^4T_{1g}$ (^4F)	Y
$^4A_{2g} \rightarrow {}^4T_{1g}$ (^4P)	Y′

The four bands Y, U, R and R′ appear in the visible part of the spectrum and their position and form are crucial for the colour perceived by the human eye. Several parameters, which are often used to characterise the electronic properties of transition-element complexes can be derived from the energies of these transitions. The most important ones are the crystal field parameter $10Dq$, which coincides with the energy of the maximum of the band U if the octahedral approximation is considered, and the Racah parameters B and C, which are calculated by the following formulae:[5]

$$B = \frac{(2\nu_1 - \nu_2)(\nu_2 - \nu_1)}{3(9\nu_1 - 5\nu_2)}$$

$$C = \frac{\nu_3 - 9B}{3}$$

Here ν_1 and ν_2 are the energies of the maxima of the U and Y bands, respectively, while ν_3 can be taken as the average of the band maxima energies of R and R′.

One has to bear in mind that specific dips denoted antiresonances may appear sometimes on the sides of the band U instead of the bands R and R′. Generally, they are explained as an effect of spin–orbit coupling of the states ^2E_g and $^2T_{1g}$ with $^4T_{2g}$. A theory developed by Fano[6,7] for atomic spectra and later adapted by Sturge *et al.*[8] for transition element electronic absorption spectra is usually used to analyse the phenomenon.[9,10] However, Neuhauser *et al.*[11] have recently developed a new more precise theory of the antiresonances, in which Fano's model have been shown to be inadequate for molecular spectra.

It should be pointed out that in addition to the spectral features discussed above, a band due to charge transfer transition could appear below 400 nm in the electronic spectra of concentrated solid solutions of Cr(III).

It is well known that chromium can be stabilized also in oxidation states 2, 4, 5 and 6 by variation of the crystal host type and the synthesis conditions. Cr(II), Cr(IV) and Cr(V) have 4, 2 and 1 electrons, respectively, in their 3d shells, thus d–d type electronic transitions are also expected to occur in them.

DOI: 10.1039/b201802k

The Cr(II) has been stabilized in several halcogenides such as ZnS, ZnSe and CdTe as well as in some glasses.[12–14] It is easily oxidised to higher oxidation states and reducing atmosphere is generally required for its synthesis. It will not be considered in the present work as all the syntheses are carried out in oxygen atmosphere.

The presence of Cr(V) has been shown in some chromates, phosphates, vanadates and silicates.[15–19] Usually, it is in tetrahedral coordination and only the electronic transition $^2E \rightarrow {}^2T_2$ is possible, resulting in a wide absorption band in the near IR region.

Cr(IV) has been obtained in multiple aluminates, gallates, silicates, germanates, chromates, fluorides, some glasses *etc.*[15] Most of the studies have been dedicated to Cr(IV)-doped forsterite[20–26] and yttrium–aluminium garnet (YAG).[27–34] Also, there is evidence for the presence of this ion in some chromium-based pigments as $CaSnSiO_5$: Cr and $CaYAlO_4$: Cr.[35–37] Usually, it coordinates four oxygen atoms and the lack of symmetry centre in the obtained tetrahedron is a premise for strong optical absorption. Three spin-allowed transitions are possible: $^3A_2(^3F) \rightarrow {}^3T_1(^3P)$, $^3A_2(^3F) \rightarrow {}^3T_1(^3F)$ and $^3A_2(^3F) \rightarrow {}^3T_2(^3F)$. The last transition causes a wide absorption band in the near IR region and could be used to detect the presence of small quantities of the ion.

Cr(VI) is the chromophore responsible for the intense yellow, orange or red hues of $PbCrO_4$ pigments.[3] In most chromates, it gives two strong absorption bands due to charge transfer transitions and their maxima are usually located at 27000 cm^{-1} and 39000 cm^{-1} (370 and 256 nm respectively).[38] In spite of the intense shades which can be obtained with this ion, it is not appropriate for use as a chromophore in pigments due to its tendency to photochemical reduction and particularly due to its carcinogenic properties.

The presence of chromium in a given oxidation state can be expected to be favoured by specific structural features such as the type of available structural sites. All of the host structures studied here possess octahedral cation sites (BO_6), with the exception of ZrO_2 (see Table 2).[39] Cr(III) has a strong affinity for six-fold coordination and its size is similar to that of the B-ions in the hosts (Al^{3+}, Sn^{4+}, Zr^{4+}, Ti^{4+}). However, non-isovalent substitution has to be considered in stannates, zirconates and titanates.

As already mentioned, Cr(IV) and Cr(V) prefer tetrahedral coordination. The spinel, garnet and sphene structures possess tetrahedral sites, but in the spinels they are much larger than the ionic radii of Cr(IV) and Cr(V).

The ionic radius of Cr(VI) is much smaller than that of the octahedral (B) and the tetrahedral (C) positions of the hosts, which together with its much higher charge makes its existence in most of the studied compounds look improbable. However, in a previous report we demonstrated the presence of Cr(VI) in YAG, synthesized by the Pechini method at temperatures as high as 1200 °C.[40] At 1400 °C, Cr(VI) was totally reduced to Cr(IV) and Cr(III), despite the oxidizing atmosphere, which suggested that Cr(VI) was stabilized at the lower temperatures by the presence of structural imperfections. Such a mechanism could also allow the stabilization of Cr(IV) and Cr(V).

Another factor influencing the colour, besides the presence and the concentration of chromium in different oxidation states, is the particular symmetry of the crystal field acting on the chromophore ions. As it can be seen from the point symmetry groups shown in Table 2, the symmetries of most of the octahedral and tetrahedral sites deviate from cubic. This deviation causes additional splitting of the energy levels and the corresponding absorption bands. For example, the splitting of the $^4T_{1g}$ and $^4T_{2g}$ levels of Cr(III) (and the respective Y and U bands) is a well known phenomenon.

It should be pointed out that the symmetries shown in Table 2 are the theoretical ones corresponding to the ideal undoped crystal structures. However, the site symmetries could change due to structural disorder induced by non-stoichiometry or by substitution. For example, reduction of the D_{3d} symmetry of the $Al(Cr)O_6$ octahedron to C_{3v} due to removal of the inversion center was suggested for spinels ($MgAl_2O_4$) doped with small chromium concentrations, based on analyses of their electronic spectra.[41] A decrease in symmetry with removal of the inversion centre was also deduced for the aluminium site with C_{3i} symmetry in garnets.[42]

The study of chromatic properties requires the use of an appropriate system to measure the colour objectively. The CIE Lab (1976) system of chromatic coordinates will be used throughout the present work for this purpose.[43] The coordinate L can vary between 0 and 100 and is interpreted as luminosity. A value of L close to zero corresponds to black while L close to 100 corresponds to white. There are no limits for the values of the coordinates a and b and they can be positive or negative depending on the colour: $a < 0$ green; $a > 0$ red; $b < 0$ blue; $b > 0$ yellow. A transformation of the Lab coordinates into

Table 2 Data related to the crystal structures of the compounds studied here

Synthesized structures	Structural type	Space group and crystal system	General formula	Coordination polyhedra and symmetry
Al_2O_3 (corundum) Cr_2O_3 (escolaite)	Corundum	$R\bar{3}c$ (167), rhombohedral	B_2O_3	BO_6, C_3
SnO_2 (cassiterite)	Rutile	$P4_2/mnm$ (136), tetragonal	BO_2	BO_6, D_{2h}
ZrO_2 (baddeleyite)	Baddeleyite	$P2_1/c$ (14), monoclinic	BO_2	BO_7, C_1
$YAlO_3$ $YCrO_3$ $CaSnO_3$ $CaTiO_3$ (perovskite)	Perovskite	$Pnma$ (62), orthorombic	ABO_3	AO_8, C_s; BO_6, C_i
$MgAl_2O_4$ (spinel) $MgCr_2O_4$ (magnesiocromite)	Spinel	$Fd\bar{3}m$ (227), cubic	AB_2O_4	AO_4, T_d; BO_6, D_{3d}
$Y_2Sn_2O_7$ $Y_2Ti_2O_7$ $Nd_2Sn_2O_7$ $Nd_2Zr_2O_7$	Pyrochlore	$Fd\bar{3}m$ (227), cubic	$A_2B_2O_7$	AO_8, D_{3d}; BO_6, D_{3d}
$Er_3Al_5O_{12}$ $Y_3Al_5O_{12}$ (YAG) $Ca_3Cr_2Si_3O_{12}$ (uvarovite)	Garnet	$Ia\bar{3}d$ (230), cubic	$A_3B_2C_3O_{12}$	AO_8, D_2; BO_6, C_{3i}; CO_4, S_4
$YCaAlO_4$	K_2NiF_4	$I4/mmm$ (139), tetragonal	A_2BO_4	AO_9, C_{4v}; BO_6, D_{4h}
$CaSnSiO_5$ (malayaite)	Sphene	$A2/a$ (15), monoclinic	$ABCO_5$	AO_7, C_2; BO_6, C_i; CO_4, C_2
$NaZr_2(PO_4)_3$ $Ca_{0.5}Zr_2(PO_4)_3$	NZP	$R\bar{3}c$ (167), rhombohedral	$AB_2(PO_4)_3$	AO_6, C_{3i}; BO_6, C_3

polar coordinates results in other two useful quantities (the coordinate L does not change). They are the chroma (c) and the hue (h), which are related to a and b by the following formulae:

$$c = \sqrt{a^2 + b^2}$$

$$h = \arctan(b/a).$$

The hue h is the closest approximation to our idea for colour saturation.

A bright red colour is characterized by $L \approx 50$, $a > 50$, $b > 30$ and $h > 50$. The visible absorption spectrum of a material of such characteristics presents very strong absorption below 600 nm and almost zero-absorption above this value, as there is a steep transition between the two regions.

Experimental section

The compositions of the samples and the conditions for their synthesis are given in Table 3. The synthesis by the Pechini method was carried out using an already established methodology.[44,45] The reagents, which were used, are shown in Table 4. Aqueous solutions were prepared, in which ethylene glycol (EG), citric acid (CA) and metal ions (ΣMe) were taken in the molar proportion ΣMe : CA : EG = 1 : 1 : 2. Heating at 120 °C under an IR lamp with simultaneous stirring caused a gradual increase of the initial viscosity of the solutions, emission of gases and vapours and, eventually, formation of amorphous brownish powders which were further used as precursors.

The solid-state reactions were carried out using the materials shown in Table 5. The raw materials taken in the corresponding stoichiometric proportion were homogenized using a planetary ball mill (Fritz Pulverisette) with agate vessels and acetone as a dispersing medium.

After drying at 100 °C, the precursors obtained by the solid-state reactions and those obtained by the Pechini method were placed in mullite crucibles and fired in several stages in an electrical furnace (Nanneti). The maximum temperature of the thermal cycles necessary to obtain pure phases was fixed between 1300–1400 °C in most cases and the soaking time was 4 h (Table 3). The phase purity of the samples was controlled by a Siemens (model D5000) diffractometer and Siemens Diffrac Plus software. The electronic absorption spectra were measured in diffuse reflectance mode employing a Perkin Elmer (model Lambda 19) spectrophotometer. The measurements were performed with a scanning step of 0.4 nm in the spectral range from 350 to 1400 nm. The chromatic coordinates CIE Lab were obtained with the same apparatus from reflectance spectra scanned in the interval 380–780 nm with a step of 1 nm and using a D_{65} illuminant.

Table 4 Raw materials for syntheses *via* the Pechini method

Precursor	Provider	Purity (%)
$Y(CH_3COO)_3 \cdot 4H_2O$	Alfa	99.9
$ErCl_3$ (anhydrous)	Strem Chemicals	99.9 Er
$Al(NO_3)_3 \cdot 9H_2O$	Prolabo	98
$Cr_3(CH_3COO)_7(OH)_2$	Aldrich	24 mass%Cr
$C_6H_8O_7$ (anhydrous citric acid)	Panreac	99.5
$(CH_2OH)_2$, ethylene glycol	Panreac	98

Table 5 Raw materials for the synthesis by solid- state reaction

Precursor	Provider	Purity (%)
Y_2O_3	Prolabo	99.5[a]
Nd_2O_3	Rhone Poulenc	98.8[a]
MgO	Merck	>97
$CaCO_3$	Merck	99
γ-Al_2O_3	Merck	99.0[a]
SnO_2	Merck	99
ZrO_2	Merck	99
TiO_2	Prolabo	>99
SiO_2	Esmaltes SA	99.8[a]
Cr_2O_3	Merck	99
$Na_2C_2O_4$	Merck	99.8
$NH_4H_2PO_4$	Merck	99

[a]Determined by X-ray fluorescence

Results

Solids containing chromium as a main component

The spectra of four solids containing chromium as a main component are shown in Fig. 1. Cr_2O_3 and $Ca_3Cr_2Si_3O_{12}$ are commercial pigments, sold under the names of Chrome Green and Victoria Green, respectively.[1,46] None of the samples exhibit bands in the NIR, which indicates that the spectra simply show Cr(III) electronic transitions. The Y and U bands are observed in the visible, and the positions of their maxima

Table 3 Synthesized samples and synthesis method

Sample	Cr content/mol	Synthesis method[a]
Cr_2O_3	2	IP
$YCrO_3$	1	SSR, 1100 + 1400 °C/2 × 4 h
$MgCr_2O_4$	2	SSR, 1100+2 × 1400 °C/2 × 4 h
$Ca_3Cr_2Si_3O_{12}$	2	IP
Al_2O_3 : Cr	0.05, 0.08	PM, 1100 + 1400 °C/2 × 4 h
$YAlO_3$: Cr	0.05, 0.2	SSR, 1100 + 1400 °C/2 × 4 h
$MgAl_2O_4$: Cr	0.05, 0.8	SSR, 1100 + 1400 + 1500 °C/3 × 4 h
$Y_3Al_5O_{12}$: Cr	0.05, 0.1, 0.15, 0.2	PM, 1100 + 1400 °C/2 × 4 h
$Er_3Al_5O_{12}$: Cr	0.1	PM, 1100 + 1400 °C/2 × 4 h
$YCaAlO_4$: Cr	0.05	SSR, 1100 + 1400 °C/2 × 4 h
SnO_2 : Cr	0.05	SSR, 1100 + 2 × 1400°C/3 × 4 h
$CaSnO_3$: Cr	0.05	SSR, 1100 + 1400 °C/2 × 4 h
$CaSnSiO_5$: Cr	0.036	SSR, 1100 + 1400 °C/2 × 4 h
$Y_2Sn_2O_7$: Cr	0.02, 0.05, 0.2, 0.5	SSR, 1100 + 1400 °C/2 × 4 h
$Nd_2Sn_2O_7$: Cr	0.02, 0.05, 0.2, 0.5	SSR, 1100 + 1400 °C/2 × 4 h
$CaTiO_3$: Cr	0.05	SSR, 1100 + 1300 °C/2 × 4 h
$Y_2Ti_2O_7$: Cr	0.05, 0.2	SSR, 1100 + 1300 °C/2 × 4 h
ZrO_2 : Cr	0.05, 0.2	SSR, 1100 + 1400 °C/2 × 4 h
$Nd_2Zr_2O_7$: Cr	0.05	SSR, 1100 + 1400 + 1500 °C/3 × 4 h
$NaZr_2(PO_4)_3$: Cr	0.05, 0.2	SSR, 400 + 1100 + 1300 °C/3 × 4 h
$Ca_{0.5}Zr_2(PO_4)_3$: r	0.2, 0.5	SSR, 400 + 1100 + 1300 °C/3 × 4 h

[a]IP = industrial pigment; SSR = solid state reaction; PM = Pechini method.

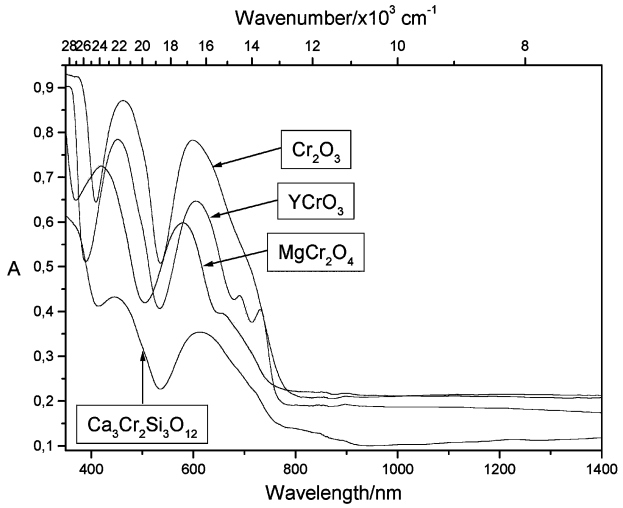

Fig. 1 Electronic absorption spectra of solids containing chromium as a main component.

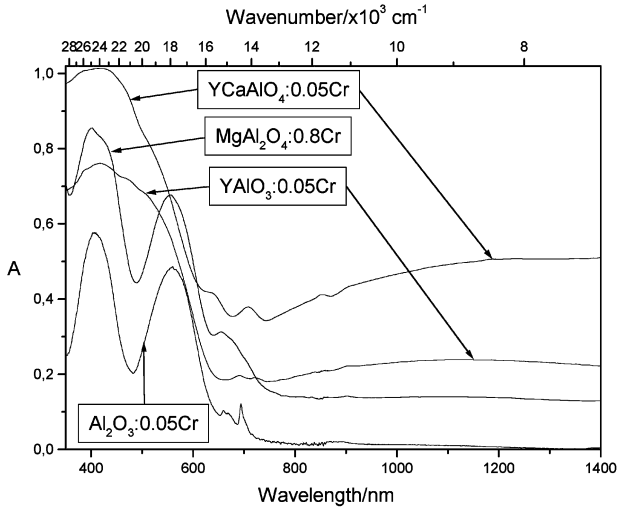

Fig. 2 Electronic absorption spectra of some solid solutions of chromium in aluminates.

Table 6 Chromatic parameters of solids containing chromium as a main component

Sample	Color	*L*	*a*	*b*	*c*	*h*
Cr_2O_3	Green	59.24	−6.25	8.72	10.72	−54.37
$YCrO_3$	Bright green	60.40	−15.23	18.80	24.19	−50.99
$MgCr_2O_4$	Greyish green	73.53	−6.41	8.36	10.53	−52.52
$Ca_3Cr_2Si_3O_{12}$	Emerald green	77.91	−8.69	11.66	14.54	−53.30

indicate the presence of Cr(III) subjected to a relatively weak octahedral field. In the spectrum of the magnesiochromite ($MgCr_2O_4$), these bands are displaced towards higher energies, which could be attributed to the contracting action of Mg(II) on the CrO_6 octahedra. The radius of Mg(II) with CN = 4 is 71 pm, which is much less than the radii of Ca(II) and Y(III) (115.9 and 126 pm, respectively, for CN = 8).[47] In addition, the R and R′ bands are clearly observed in the spectra of $YCrO_3$ and $MgCr_2O_4$, while they only form a shoulder in the spectra of Cr_2O_3 and $Ca_3Cr_2Si_3O_{12}$. The bands at 350–400 nm are assigned to the charge-transfer transition from the oxygen 2p valence band to the chromium 3d conduction band.

As Table 6 shows, all four chromium oxides present similar green shades, their *a*-coordinates being negative and their hue values (*h*) varying to a very limited extent. This is typical for octahedrally coordinated Cr(III) in relatively relaxed structures, *i.e.* the case of a weak crystal field.

Solid solutions of Cr in aluminates

The spectra of four solid solutions of chromium in aluminates are shown in Fig. 2. The spectra of the chromium doped erbium–aluminium and yttrium–aluminium garnets are shown separately in Fig. 3. The spectra of Al_2O_3 and $MgAl_2O_4$ doped with small concentrations of chromium differ from the spectra of Cr_2O_3 and $MgCr_2O_4$ by the higher energy of the Y and U bands. This can be explained by the smaller ionic radius of Al(III) compared to Cr(III) (67.5 pm *vs.* 75.5 pm, respectively, for CN = 6)[47] which causes an increase in the octahedral crystal field strength when chromium is substituted by aluminium. Nevertheless, the spectra of $YAlO_3$ and $YCaAlO_4$ can not be explained only by the presence of Cr(III). The wide bands in the NIR and the complex structure of the absorption in the visible are indications for the presence of Cr(IV). The presence of Cr(V) can not be excluded on the basis of these observations only. Since neither $YAlO_3$ nor $YCaAlO_4$ have tetrahedral sites available these ions are expected to enter into interstitial sites. The superposition of Cr(IV) bands with Cr(III) bands results in

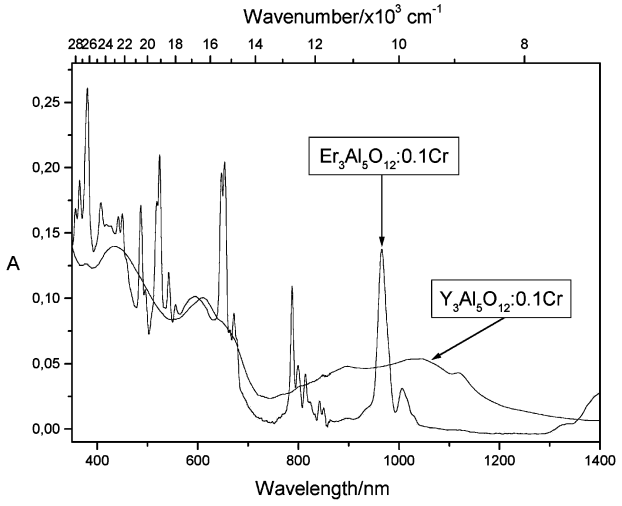

Fig. 3 Electronic absorption spectra of solid solutions of chromium in yttrium–aluminium garnet and erbium–aluminium garnet.

a strong optical absorption in the visible, and consequently, in very intense hues which are red in the case of $YAlO_3$ (see Table 7).

A band centered at about 1020 nm in the spectrum of $Y_3Al_5O_{12}$: 0.1Cr shown in Fig. 3 also reveals the presence of Cr(IV). As it is expected to replace Al(III) in the tetrahedral garnet sites and no element is included in the structure to act as a charge compensator, an alternative mechanism of compensation is suggested, consisting in the formation of cation vacancies. The positions of the U and Y bands of Cr(III) correspond to a weak crystal field. The substitution of the yttrium in the YAG for erbium causes the appearance of several narrow peaks due to f–f transitions, which overlap the chromium spectrum. In spite of this, the energy of the $^4A_{2g} \rightarrow {}^4T_{2g}$ transition can be determined and is about 400 cm^{-1} higher than that corresponding to YAG, *i.e.* the crystal field is slightly stronger but it still remains weak. The small increase is due to the slightly smaller ionic radius of erbium (114.4 pm) compared to yttrium (115.9 pm). The colour of Er^{3+} itself is pink but the crystal field acting on Cr(III) is not sufficiently intense as to lead to a red shade.

The chromatic parameters of the aluminate samples are compared in Table 7. The chroma parameters (*c*) of the $YAlO_3$: Cr and $CaYAlO_4$: Cr samples are substantially higher than those of the other samples, as a consequence of the intense

Table 7 Chromatic parameters of solid solutions of chromium in aluminates

Sample	Cr content/mol	Color	L	a	b	c	h
Al_2O_3	0.05	Pink	82.11	6.82	−0.02	6.82	−0.168
	0.08	Pink	77.07	7.70	−0.11	7.70	−0.82
$YAlO_3$	0.05	Pink	73.67	15.16	15.33	21.56	45.32
	0.20	Red	57.75	16.73	10.38	19.69	31.82
$MgAl_2O_4$	0.05	Light pink	91.57	3.73	0.74	3.80	11.2
	0.80	Pink	71.79	3.96	6.35	7.48	58.0
$Y_3Al_5O_{12}$	0.05	Pale green	97.56	−2.71	5.85	6.45	−65.14
	0.10	Pale green	97.22	−5.68	6.97	8.99	−50.8
	0.15	Green	95.14	−7.55	8.19	11.1	−47.3
	0.20	Green	84.78	−5.44	6.86	8.76	−51.6
$Er_3Al_5O_{12}$	0.10	Greenish grey	91.74	−0.51	3.97	4.00	−82.7
$YcaAlO_4$	0.05	Orange	68.18	11.74	21.18	24.21	61.00

absorption in the visible part of their spectra. However, the colour of $CaYAlO_4$: Cr has a high yellow component (b) which coincides with data reported by Olazcuaga.[48] There are commercial pink pigments based on the solid solutions of chromium in alumina and spinels in spite of their relatively low colour saturation.

Solid solutions of chromium in stannates

The spectra of three compounds of the ternary system CaO–SnO_2–SiO_2 doped with chromium are shown in Fig. 4. These compounds, particularly the cassiterite (SnO_2) and the malayaite ($CaSnSiO_5$), are of primary importance for the ceramic pigments industry as combined in different proportions they form intensely coloured pinks and violets.[49,50] The spectra of these two chromium-doped structures are very similar in the visible region. Particularly interesting are the absorption bands around 700 nm which can be assigned again to the spin-forbidden transitions of Cr(III) already discussed. They are much more intense than in other structures and this fact can be attributed to the strong distortion of the corresponding octahedral sites.

There is a band in the near-IR part of the spectrum of the chromium-doped malayaite (at 1200 nm), which is not found in cassiterite. Once again it can be attributed to Cr(IV) and in this case this ion can be stabilized in the tetrahedral SiO_4 site. There are no such sites in the perovskite $CaSnO_3$ but still it has a similar, though less intense band, whose maximum appears at about 1200 nm.

The spectra of two chromium solid solutions in tin pyrochlores are shown in Fig. 5. The spectrum of the neodymium variety apparently consists of bands caused by neodymium f–f

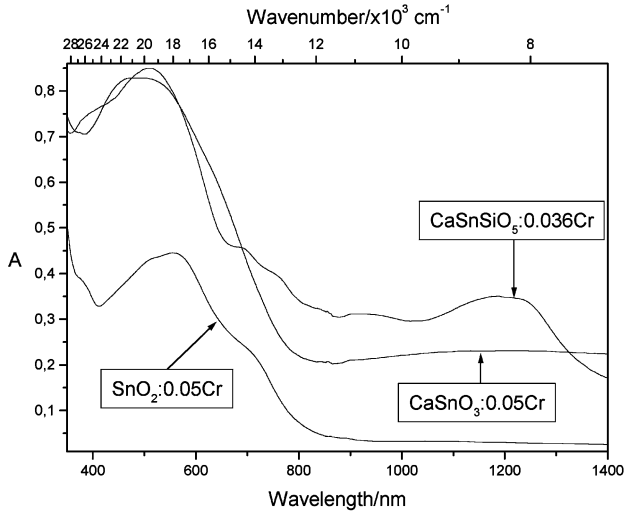

Fig. 4 Electronic absorption spectra of solid solutions of chromium in three tin-containing oxides.

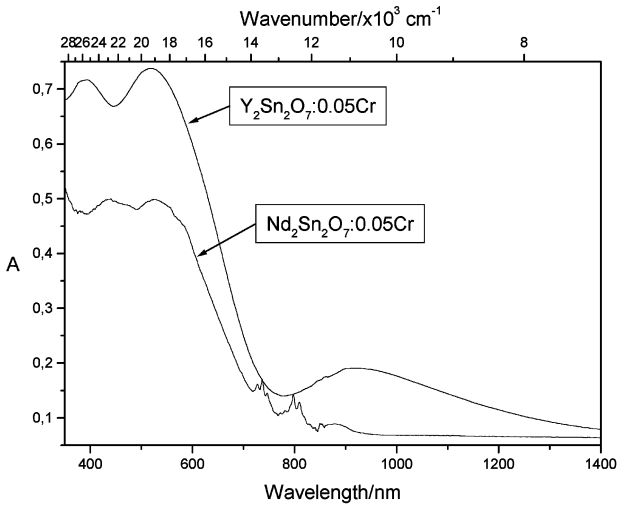

Fig. 5 Electronic absorption spectra of solid solutions of chromium in two tin-containing pyrochlores.

transitions superimposed on Cr(III) bands. A new band appears in the spectrum of the yttrium pyrochlore peaking at about 920 nm, which can only be explained by the presence of Cr(V) or Cr(IV) in interstitial sites. The spin allowed bands of Cr(III) in the visible are displaced towards higher energies with respect to those belonging to the neodymium pyrochlore, as a result of Y^{3+} having a smaller ionic radius than Nd^{3+} (115.9 pm *vs.* 124.9 pm, respectively; CN = 8).[47] This same difference could be the factor responsible for the stabilization of chromium in one or another oxidation state.

The colour coordinates shown in Table 8 indicate that all stannate solid solutions present red shades (a is positive), at the low chromium concentrations present. The chromatic purity (c) is particularly high in the pyrochlore and the malayaite-based solid solutions.

Table 8 Chromatic parameters of the solid solutions of chromium in stannates

Sample	Cr content/mol	Color	L	a	b	c	h
SnO_2	0.05	Violet	68.04	7.72	−4.34	8.85	−29.34
$CaSnO_3$	0.05	Maroon	46.36	8.94	3.74	9.69	22.70
$CaSnSiO_5$	0.036	Pink	50.18	11.45	5.53	12.71	25.78
$Y_2Sn_2O_7$	0.02	Pink	55.28	12.22	1.75	12.34	8.15
	0.05	Pink	52.24	12.10	1.70	12.22	8.00
	0.2	Brown	45.96	8.66	1.78	8.84	11.61
	0.5	Brown	41.72	7.01	2.08	7.31	16.53
$Nd_2Sn_2O_7$	0.02	Pinkish	72.64	6.56	6.51	9.24	44.78
	0.05	Pinkish	72.41	6.97	3.22	7.68	24.79
	0.2	Brown	58.17	7.34	3.16	7.99	23.29
	0.5	Brown	57.40	4.95	5.58	7.46	48.42

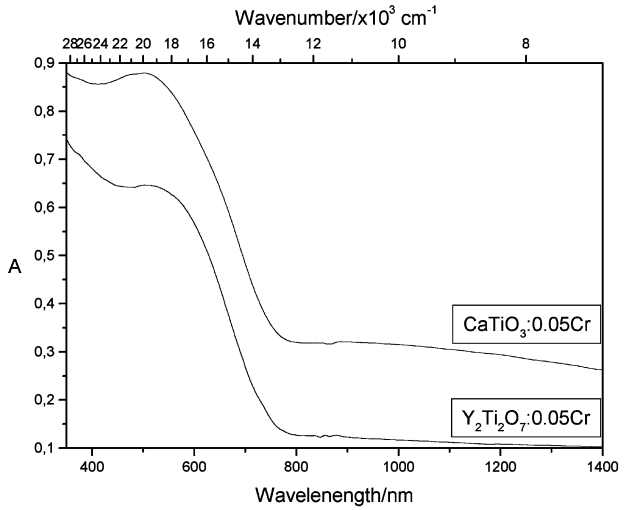

Fig. 6 Electronic absorption spectra of solid solutions of chromium in two titanium-containing oxides.

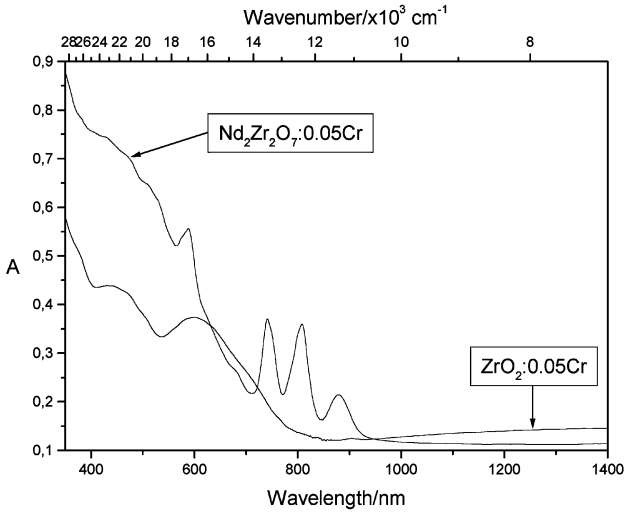

Fig. 7 Electronic absorption spectra of solid solutions of chromium in zirconia and neodymium–zirconium pyrochlore.

Table 9 Chromatic parameters of solid solutions of chromium in titanates

Sample	Cr content/ mol	Color	*L*	*a*	*b*	*c*	*h*
$CaTiO_3$	0.05	Brownish pink	45.25	7.88	4.15	8.91	27.77
$Y_2Ti_2O_7$	0.05	Brownish pink	56.34	7.00	3.94	8.03	29.37
	0.2	Brownish pink	46.59	5.74	2.48	6.25	23.37

Solid solutions of chromium in titanates

Two titanate hosts were studied and their spectra are shown in Fig. 6. There seems to be no evidence that they may contain chromium in oxidation states four or five but a shoulder at 400 nm in the spectrum of the chromium-doped pyrochlore points out that a charge transfer transition occurs either in Cr(VI) or between chromium and titanium. Charge transfer transitions are a common phenomena in titanium-containing oxides and are pointed out as the cause of the dark brown or black shades of minerals such as rutile, melanite, tourmaline and some micas.[51]

As Table 9 shows, these solid solutions have low chromatic purity (*c*) and this makes them inappropriate for use as pigments.

Solid solutions of chromium in zirconium-containing compounds

The last group of studied samples is based on chromium solid solutions in zirconium-containing hosts. A spectrum of zirconia and a spectrum of neodymium–zirconium pyrochlore, both doped with chromium, are shown in Fig. 7. The latter is a superposition of the bands originated by Nd(III) f–f, Cr(III) d–d and Cr(VI) CT (charge transfer) transitions. The spectrum of the chromium-doped zirconia manifests the presence of Cr(III) in a weak octahedral field, as well as chromium in higher oxidation states. The shoulder between 350 and 400 nm is an indication for the presence of Cr(VI), as in the other spectra, and the weak and wide absorption band with a maximum at 1390 nm is attributable to Cr(IV) or Cr(V). The zirconium in the ideal zirconia structure is seven-coordinated, thus the octahedral and the tetrahedral coordination of the dopant cations can be expected to be achieved by formation of structural defects.

The spectra of chromium in two phosphates with the so-called NZP structure were also studied in order to verify the information given in a report, according to which pink shades could be obtained in similar solid solutions.[52] As can be seen in Fig. 8, only Cr(III) bands are present, and their positions

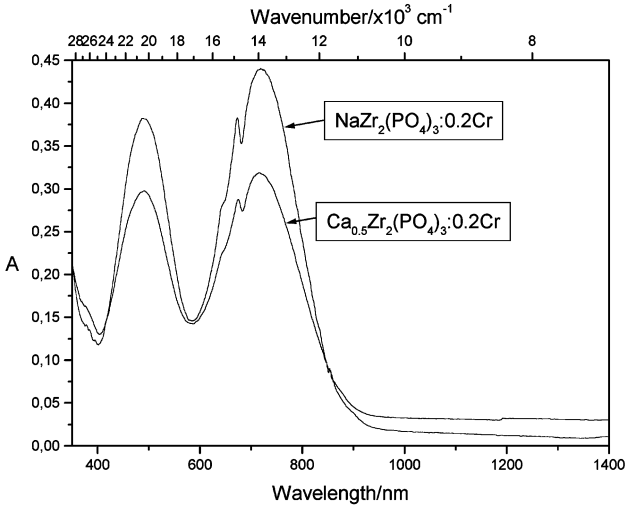

Fig. 8 Electronic absorption spectra of solid solutions of chromium in two NZP-type structures.

correspond to an extremely weak crystal field. The positions of the absorption maxima of the Y and U bands are very similar to those reported by Alamo and Cuadrado.[52] However, a thorough inspection of the high-energy side of the U band shows that a case of Fano's antiresonances is present here in form of two dips, which can be attributed to spin–orbit coupling of the ^2E_g and $^2T_{1g}$ states with the state $^4T_{2g}$. Thus, a more complicated analysis should be carried out in order to determine the energies of the corresponding transitions.

The colour coordinates of all studied chromium solid solutions in zirconates are given in Table 10. The values of *L* and *c* indicate that most colours are very pale. The high *b* value of the neodimium–zirconium pyrochlore confirms the suggestion that Cr(VI) is present. The NZP structure proves to be an inadequate matrix for developing pink chromium pigments. However, it is interesting to point out that it exhibits a strong thermochromic effect consisting in beige-to-violet chromatic change when heated.

Discussion

The energies of the transitions $^4A_{2g} \rightarrow {}^4T_{1g}$, $^4A_{2g} \rightarrow {}^4T_{2g}$, $^4A_{2g} \rightarrow {}^2E_g$ and $^4A_{2g} \rightarrow {}^2T_{1g}$ of Cr(III) could be determined directly only in some cases since the corresponding bands were often overlapped between each other or by Cr(IV) bands. The energies

Table 10 Chromatic parameters of solid solutions of chromium in zirconium-containing compounds

Sample	Cr content/ mol	Color	L	a	b	c	h
ZrO_2	0.05	Green	81.34	−2.23	5.75	6.17	−68.80
	0.2	Green	77.65	−3.37	4.95	5.99	−55.75
$Nd_2Zr_2O_7$	0.05	Pinkish beige	65.38	8.36	8.40	11.85	45.14
$NaZr_2(PO_4)_3$	0.05	Light beige	85.50	−0.94	5.35	5.43	−80.03
	0.2	Light beige	87.14	7.15	3.71	8.06	27.42
$Ca_{0.5}Zr_2(PO_4)_3$	0.2	Light beige	83.69	6.21	4.35	7.58	35.01
	0.5	Green	74.27	−3.02	6.05	6.76	−63.47

of the last two transitions could be determined in some samples from the minima of the second derivative of their spectra. The energies of the transitions and the Racah parameters calculated from them are given in Table 11.

As it can be seen, the energy of the spin allowed transition $^4A_{2g} \rightarrow {}^4T_{2g}$ of Cr(III), which theoretically coincides with the crystal field parameter $10Dq$, presents wide variations ranging from about 16300 to about 19900 cm^{-1} depending on the structure of the host. The NZP structure presents a very low value of $10Dq = 14000$ cm^{-1}, which is explained by the influence of the highly covalent phosphor atoms.

For a given structure, the value of $10Dq$ is practically unaffected by the chromium concentration, except for the cases where complete series of solid solutions are possible, for example, Al_2O_3–Cr_2O_3, $MgAl_2O_4$–$MgCr_2O_4$ and $YAlO_3$–$YCrO_3$. Consequently, substantial colour changes (such as from red to green and *vice versa*) can be expected only if the chromium is very soluble in the matrix or, ideally, if a complete series of solid solutions exists.

The energy of the spin allowed transition $^4A_{2g} \rightarrow {}^4T_{1g}$ varies between 21700 and 25600 cm^{-1} according to the crystal structure type (the NZP structure again shows an exception with a value of 20400 cm^{-1}). The energies of the spin-forbidden transitions $^4A_{2g} \rightarrow {}^2E_g$ and $^4A_{2g} \rightarrow {}^2T_{1g}$ present much smaller variations, the former ranging between 13700–14700 and the latter between 14400–15220 cm^{-1}. However, their intensities do vary to a great extent depending on the structure, which evidences their importance for the colour.

The measured chroma (c) of the solid solutions were generally less than 10 with only 6 from a total of 17 synthesized solid solutions developing shades with $c > 10$. In five of these six solid solutions, both experimental and reference data indicate the presence of Cr(IV). This correlation can be explained by the fact that the optical transitions of Cr(IV) have very high probability due to the lack of a symmetry centre in its complexes (tetrahedral), which causes partial mixing of its d-orbitals with the p-orbitals of the ligands. Some of the bands overlap the Cr(III) bands in the visible thus causing strong absorption and intense colouration. The only one solid solution with $c > 10$ in which Cr(IV) is not detected is $Nd_2Zr_2O_7$: 0.05Cr whose intense pinkish-yellow shade is attributed to Cr(VI). Samples which present IR bands are listed in Table 12.

Table 12 Solid solutions with absorption bands in the NIR

Composition	NIR bands/cm^{-1}
$Y_3Al_5O_{12}$: 0.05Cr	8900, 9600, 11200
$YAlO_3$: 0.05Cr	8420, 8890
$Y_2Sn_2O_7$: 0.05Cr	10800
$CaSnO_3$: 0.05Cr	8250, 11000
$CaSnSiO_5$: 0.036Cr	8400, 11000
$CaYAlO_4$: 0.05Cr	7260, 8420
ZrO_2 : 0.05Cr	7200

The existence of sites with appropriate size and geometry is required in order to stabilize the chromophores in the host structures. The substitution of Al(III) for Cr(III) is easily explained considering their equal charges and coordination numbers, as well as their similar ionic sizes. However, the substitution of Sn(IV), Zn(IV) or Ti(IV) for Cr(III) involves the formation of defects due to the necessity of charge compensation. Some structures such as the baddeleyite (m-ZrO_2) do not posses octahedral sites necessary for the substitution by Cr(III), thus their creation involves formation of oxygen vacancies. On the other hand, the presence of Cr(VI) and Cr(IV) supposes the existence of tetrahedral sites of appropriate size. In some structures where these ions appear, for example, $Y_3Al_5O_{12}$ and $CaSnSiO_5$, this requirement is satisfied, while in others such as $YAlO_3$, $YCaAlO_4$ and $Y_2Sn_2O_7$, the existence of tetrahedral positions requires the consideration of defects. Our current studies by neutron diffraction on pyrochlore solid solutions $Y_2Sn_2O_7$: Cr confirm this hypothesis, showing an increasing concentration of oxygen vacancies when increasing the total chromium concentration. It is inevitable that the defects originate distortions in the structures. This may cause a change in the symmetry of the surroundings of the chromophore and therefore the colour.

Acknowledgements

The authors are grateful to Prof. Xermán de la Fuente from ICMA-CSIC, Zaragoza (Spain) for helpful discussions. Also,

Table 11 Racah parameters B and C and energies E (cm^{-1}) of the electronic transitions of Cr(III) (where identified) from the ground state $^4A_{2g}$

Composition	$E(^4T_{1g})$	$E(^4T_{2g}) = 10Dq$	$E(^2T_{1g})$	$E(^2E_g)$	B	C
Al_2O_3 : 0.05Cr	24700	17860	15200	14400	674.7	2909
Cr_2O_3	21700	16700	(13900)[a]		466.5	3234
ZrO_2 : 0.05Cr	23100	16700	—	—	631.4	—
$YalO_3$: 0.05Cr	—	—	14500	14000	—	—
$YCrO_3$	22100	16500	14400	13700	535.4	3077
$CaTiO_3$: 0.05Cr	—	19900	(15200)[a]	—	—	—
$MgAl_2O_4$: 0.8Cr	25000	18000	15220	(14700)[a]	693.7	2906
$MgCr_2O_4$	23800	17300	15200	(14400)[a]	637.6	3020
$Y_2Sn_2O_7$: 0.05Cr	25600	19300	—	—	597.4	—
$Nd_2Sn_2O_7$: 0.05Cr	22900	19000	—	—	347.4	—
$Y_2Ti_2O_7$: 0.05Cr	—	19600	—	—	—	—
$Er_3Al_5O_{12}$:0.1Cr	—	16800	—	—	—	—
$Y_3Al_5O_{12}$: 0.1Cr	23000	16400	(14900)[a]	—	661.3	2983
$Ca_3Cr_2Si_3O_{12}$	22400	16300	(14400)[a]	(13800)[a]	597.7	2907
$NaZr_2(PO_4)_3$: 0.2Cr	20400	13900	—	—	694.1	
$Ca_{0.5}Zr_2(PO_4)_3$: 0.2Cr	20400	14000	—	—	675.5	

[a]The energies of the states $^2T_{1g}$ and ^2E_g given in parentheses were evaluated using the second derivative of the spectra.

one of the authors (R. S. P.) would like to acknowledge the financial support provided by AECI.

References

1 R. Eppler and D. Eppler, *Ceram. Eng. Sci. Proc.*, 1994, **15**, 281–288.
2 *Safe Handling of Pigments*; Color Pigments Manufacturers Association Inc. (CPMA), Alexandria, Virginia, 1993.
3 G. Buxbaum, *Industrial Inorganic Pigments*, 2nd edn., Wiley-VCH, London, 1998.
4 S. Sugano, Y. Tanabe and H. Kamimura, *Multiplets of Transition Metal Ions in Crystals*, Academic Press, New York, 1970.
5 Y. Tanabe and S. Sugano, *J. Phys. Soc. Jpn.*, 1954, **9**, 753–766; Y. Tanabe and S. Sugano, *J. Phys. Soc. Jpn.*, 1954, **9**, 766–779.
6 U. Fano, *Phys. Rev.*, 1961, **124**, 1886.
7 U. Fano and J. Cooper, *Phys. Rev.*, 1965, **137**, 1364.
8 M. Sturge, H. Guggenheim and M. Price, *Phys. Rev. B: Condens. Matter*, 1970, **2**, 2459.
9 A. Lempicki, L. Andrews, S. Nettel and B. McCollum, *Phys. Rev. Lett.*, 1980, **44**, 1234–1237.
10 U. Rodríguez-Mendoza, V. Rodríguez, V. Lavin, I. Martín and P. Nuñez, *Spectrochim. Acta, Part A*, 1999, **55**, 1319–1322.
11 D. Neuhauser, T. Park and J. Zink, *Phys. Rev. Lett.*, 2000, **85**, 5304–5307.
12 R. Renz and H. Schulz, *J. Phys. C.*, 1983, **16**, 4917–32.
13 V. Davis, X. Wu, U. Hömmerich, K. Grasza, S. Trivedi and Z. Yu, *J. Lumin.*, 1997, **72**, 281–283.
14 E. Pretorius, R. Snellgrove and A. Muan, *J. Am. Ceram. Soc.*, 1992, **75**, 1378–81.
15 E. Zharikov and V. Smirnov, *Wide-Gap Luminescent Materials: Theory and Applications*, ed. S. Rotman, Kluwer Academic Publishers, ch. 1, 1997.
16 Y. Aoki and H. Konno, *J. Solid State Chem.*, 2001, **156**, 370–378.
17 I. Arcon, B. Mirtic and A. Kodre, *J. Am. Ceram. Soc.*, 1998, **81**, 222–24.
18 B. Mitric, A. Fajgelj, K. Lutar, M. Schara and V. Kaucic, *J. Am. Ceram. Soc.*, 1992, **75**, 2184–88.
19 D. Reinen, U. Kesper, M. Atanasov and J. Roos, *Inorg. Chem.*, 1995, **34**, 184–192.
20 V. Petricevic, S. Gayen and R. Alfano, *Opt. Lett.*, 1989, **14**, 612.
21 V. Petricevic, S. Gayen and R. Alfano, *Appl. Phys. Lett.*, 1988, **53**, 2590.
22 W. Lu, B. Tissue and W. Yen, *J. Cryst. Growth*, 1991, **109**, 329–333.
23 B. Hu, H. Zhu and P. Deng, *J. Cryst. Growth*, 1993, **128**, 991–995.
24 Y. Yamaguchi, K. Yamagushi and Y. Nobe, *J. Cryst. Growth*, 1993, **128**, 996–1000.
25 D. Calistru, W. Wang, V. Petricevic and R. Alfano, *Phys. Rev. B: Condens. Matter*, 1995, **51**, 14980–86.
26 N. Kuleshov, V. Shcherbitsky, V. Mikhailov, S. Hartung, T. Danger, S. Kück, K. Petermann and G. Huber, *J. Lumin.*, 1997, **75**, 319–325.
27 B. Tissue, W. Jia, L. Lu and W. Yen, *J. Appl. Phys.*, 1991, **70**, 3775–77.
28 S. Kück, U. Pohlmann, K. Petermann, G. Huber and T. Schönherr, *J. Lumin.*, 1994, **60 & 61**, 192–196.
29 H. Eilers, U. Hömmerich, S. Jacobsen and W. Yen, *Phys. Rev. B: Condens. Matter*, 1994, **49**, 15505–13.
30 A. Ikesue, K. Yoshida and K. Kamata, *J. Am. Ceram. Soc.*, 1996, **79**, 507–509.
31 M. Brik and V. Zhorin, *J. Lumin.*, 1997, **72**, 149–151.
32 S. Markgraf, M. Pangborn and R. Dieckermann, *J. Cryst. Growth*, 1997, **180**, 81–84.
33 D. Jun, D. Peizhen and X. Jun, *J. Cryst. Growth*, 1999, **203**, 163–167.
34 B. Brickeen and W. Ching, *J. Appl. Phys.*, 2000, **88**, 3073–75.
35 A. Heyns and P. Harden, *J. Phys. Chem. Solids*, 1999, **60**, 277.
36 Ch. Chaumont, G. Le Flem and P. Hagenmuller, *Z. Anorg. Allg. Chem.*, 1980, **470**, 18–24.
37 I. Zvereva, L. Zueva, F. Archaimbault, M. Crespin, J. Choisnet and J. Lecomte, *Mater. Chem. Phys.*, 1997, **48**, 103–110.
38 M. Wolfsberg and L. Helmholz, *J. Chem. Phys.*, 1952, **20**, 837.
39 *International Tables for Crystallography*, ed. T. Hahn, Kluwer Academic Publishers, Dordrecht, Boston, London, 1992, vol. A.
40 R. Pavlov, V. Blasco, E. Cordoncillo, P. Escribano and J. Carda, *Bol. Soc. Esp. Ceram. Vidr.*, 2000, **39**, 609–615.
41 K. Ikeda, Y. Nakamura, K. Masumoto and H. Shima, *J. Am. Ceram. Soc.*, 1997, **80**, 2672–76.
42 A. Marshall, K. O'Donnell, M. Yamaga, B. Henderson and B. Cockayne, *Appl. Phys. A*, 1990, **50**, 565–572.
43 CIE, *Recommendations on Uniform Color Spaces, Color Difference Equations, Psychometrics Color Terms*. Suplement No.2 of CIE Publ. No.15 (E1-1.31) 1971, Bureau Central de la CIE, Paris, 1978.
44 M. P. Pechini, *US Pat.*, 3330697, 1967.
45 M. Kakihana, *J. Sol–Gel Sci. Tecnol.*, 1996, **6**, 7–55.
46 J. Carda, G. Monrós, M. Tena and P. Escribano, *J. Am. Ceram. Soc.*, 1994, **77**, 2097–106.
47 R. Shannon and C. Prewitt, *Acta Crystallogr., Sect.B*, 1969, **25**, 925–945.
48 R. Olazcuaga, R*ed Pigments with Transition or Rare Earth Elements for High Temperature Ceramics; in Nuevos Productos y Tecnologías de Esmaltes y Pigmentos Cerámicos*, ed. J. Rincón, J. Carda and J. Alarcón, Faenza Editrice Iberica, Castellón, Spain, 1991.
49 R. Stefani, E. Longo, P. Escribano, E. Cordoncillo and J. Carda, *Am. Ceram. Soc. Bull.*, 1997, **76**, 61–64.
50 R. Stefani, E. Longo, P. Escribano, E. Cordoncillo and J. Carda, *Key Eng. Mater.*, 1997, **132**, 277–280.
51 R. Moore and W. White, *Am. Mineral.*, 1971, **56**, 826–840.
52 M. Cuadrado and J. Alamo, *Br. Ceram. Trans. J.*, 1988, **87**, 141–144.